JCTC Journal of Chemical Theory and Computation

ARTICLE

pubs.acs.org/JCTC

Charge-Transfer-Like $\pi \rightarrow \pi^*$ Excitations in Time-Dependent Density Functional Theory: A Conundrum and Its Solution

Natalia Kuritz,[†,§] Tamar Stein,[‡,§] Roi Baer,[*,‡] and Leeor Kronik[*,†]

[†]Department of Materials and Interfaces, Weizmann Institute of Science, Rehovoth 76100, Israel

[‡]Fritz Haber Center for Molecular Dynamics, Institute of Chemistry, Hebrew University, Jerusalem 91904, Israel

ABSTRACT: We address the conundrum posed by the well-known failure of time-dependent DFT (TDDFT) with conventional functionals for "charge-transfer-like" excitations in oligoacenes. We show that this failure is due to a small spatial overlap in orbitals obtained from the underlying single-electron orbitals by means of a unitary transformation. We further show that, as in true charge-transfer excitations, this necessarily results in failure of linear-response TDDFT with standard functionals. Range-separated hybrid functionals have been previously shown to mitigate such errors but at the cost of an empirically adjusted range-separation parameter. Here, we explain why this approach should succeed where conventional functionals fail. Furthermore, we show that optimal tuning of a range-separated hybrid functional, so as to enforce the DFT version of Koopmans' theorem, restores the predictive power of TDDFT even for such difficult cases, without any external reference data and without any adjustable parameters. We demonstrate the success of this approach on the oligoacene series and on related hydrocarbons. This resolves a long-standing question in TDDFT and extends the scope of molecules and systems to which TDDFT can be applied in a predictive manner.

I. INTRODUCTION

Time-dependent density functional theory (TDDFT) is an approach for the calculations of excited-state properties that is based on mapping the time-dependent Schrödinger equation into an equivalent set of Schrödinger-like equations for fictitious, noninteracting electrons.[1−5] In principle, TDDFT is an exact theory. In practice, the above-mentioned mapping relies on an exchange−correlation potential, which is a functional of the electron density, but whose exact dependence on the density is unknown. The success or failure of TDDFT therefore hinges entirely on the availability of practical and reliable approximate forms for the exchange−correlation potential.

Almost all practical TDDFT calculations are performed using the adiabatic approximation, i.e., assuming that at each moment in time the exchange−correlation potential depends only on the contemporaneous density. In local or semilocal approximations, such as the local density approximation (LDA)[6] or the generalized gradient approximation (GGA),[7] it is further assumed that at each point in space the exchange−correlation potential depends only on the density at this point (in LDA) or also on its gradient (in GGA). In hybrid functionals (e.g., B3LYP,[8,9] a functional of great popularity in organic chemistry), a fraction of a nonlocal Fock-exchange operator is also used. Linear-response TDDFT calculations with these standard approximations have proven to be a remarkably accurate tool for first principles calculations of valence excitations in broad classes of molecular and nanoscale systems.[2,4,10−13] Despite this impressive success, lingering doubts about the true predictive power of TDDFT using these approximations remain, because failures are sometimes encountered in simple and seemingly straightforward scenarios.

Perhaps the best-known example of a failure without an obvious root in the underlying formalism is the prediction of $\pi \rightarrow \pi^*$ singlet excitation energies in the oligoacene series, $C_{2+4n}H_{4+2n}$ (n = 2−6).[14] The two lowest such excitations, usually labeled ^1L_a and ^1L_b, a notation due to Platt,[15] differ in character. ^1L_a is dominated by the highest occupied molecular orbital (HOMO)−lowest unoccupied molecular orbital (LUMO) transition and is short-axis polarized. ^1L_b is dominated by a mixture of two transitions, usually the HOMO-1−LUMO and HOMO−LUMO+1 ones, and is long-axis polarized. Grimme and Parac noticed that whereas the ^1L_b excitation energy is reasonably well-predicted by TDDFT using a GGA functional (BP86)[16,17] and very-well predicted by using a hybrid functional (B3LYP)[8,9], the ^1L_a excitation energy is consistently and substantially underestimated by either functional. These conclusions have been confirmed since by numerous additional studies and also extended to related systems exhibiting $\pi \rightarrow \pi^*$ excitations, notably nonlinear polyaromatic hydrocarbons (see, e.g., refs 5 and 18−23). They are underscored in Figure 1, where TDDFT with both BP86 and B3LYP are compared to the approximate coupled-cluster singles and doubles method (CC2) results of Grimme and Parac,[14] which we take as a reference.[24] For the ^1L_b excitation energy, the mean error between the TDDFT-B3LYP and the CC2 results across the naphthalene to hexacene series is a satisfactory 0.04 eV. But for the ^1L_a excitation energy, TDDFT-B3LYP consistently underestimates the CC2 results, with an unsatisfactory mean error of 0.47 eV.

A different arena where linear-response TDDFT calculations with the same approximate functionals are known to fail is the prediction of charge-transfer excitation energies.[25−27] These excitations are characterized by a small spatial overlap between the initial and the final orbital of the excited electron. Here and throughout, we define the spatial overlap between two orbitals, O_{12}, as the inner product of the moduli of two orbitals

Received: April 22, 2011
Published: June 22, 2011

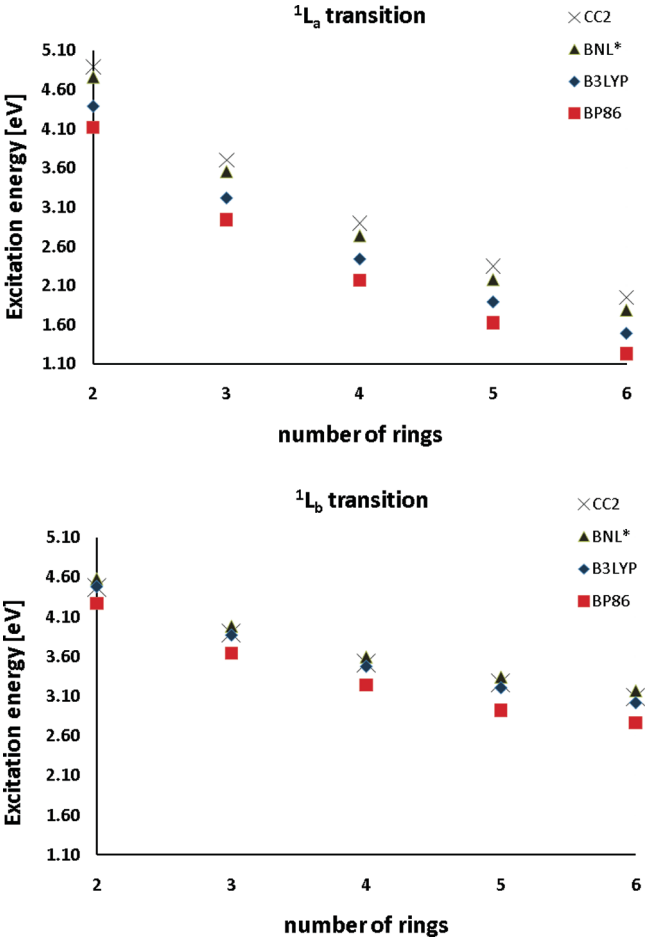

Figure 1. Excitations energies of the ^1L_a (a) and ^1L_b (b) transitions in the oligoacene series, $C_{2+4n}H_{4+2n}$ (n = 2 to 6). TDDFT data obtained with the BP86 GGA functional (red squares), the B3LYP standard hybrid functional (blue diamonds), and the optimally tuned BNL range-separated hybrid functional (green triangles) are compared to reference CC2 values, taken from ref 14 (black '×' signs).

ψ_1 and ψ_2,[28] namely

$$O_{12} \equiv \langle|\psi_1||\psi_2|\rangle \tag{1}$$

One perspective for this failure, given by Dreuw and Head-Gordon,[25] is that it is a direct consequence of the above-defined small spatial overlap. For such a case, exact (Fock) exchange would yield the correct electron−hole attraction term, but Fock exchange is completely absent in semilocal functionals and only a fraction of it is present in standard hybrid functionals. Therefore, at least within adiabatic linear response theory,[29] they cannot be expected to yield the correct result.

In the past few years, many studies[30−42] have shown that the charge-transfer excitation problem can be remedied with the aid of a novel class of hybrid functionals known as range-separated hybrid (RSH) functionals.[43−49] In this class of functionals, the repulsive Coulomb potential is split into a long-range (LR) and short-range (SR) term, e.g., via $r^{-1} = r^{-1}\,\mathrm{erf}(\gamma r) + r^{-1}\mathrm{erfc}(\gamma r)$. The components are treated differently in the generation of the exchange term. The SR exchange is represented by a local potential, typically derived from a GGA expression, whereas the LR part is treated via an "explicit" or "exact" exchange term. This affords a natural way for providing the missing Fock term for long-ranged interactions between nonspatially overlapping orbitals while maintaining the compatibility between exchange and correlation for short-ranged interactions.

Very recently, Wong and Hsieh[50] have shown that use of a RSH functional also cures the above-discussed underestimate of ^1L_a excitation energies in oligoacenes and still performs well for ^1L_b excitations energies. Subsequently, Richard and Herbert[51] have confirmed these findings and extended them to a wide range of nonlinear polyaromatic hydrocarbons. This success is not at all trivial because ^1L_a excitations are certainly not charge-transfer excitations in the sense of eq 1, and even more refined quantitative measures of the nature of the excitation[28] clearly identify them as regular valence excitations.[19,50−52] This has led Richard and Herbert[51] to postulate that such excitations possess a "charge-transfer character in disguise" and to pose two important and related questions, which we paraphrase as follows: (1) How can this charge-transfer-like character be detected a priori? and (2) In the absence of accurate (ab initio or experimental) reference data, can we really trust TDDFT to have predictive power in such cases?

In this article, we propose a solution to this conundrum. First, we show that the elusive charge-transfer-like characteristics are due to a small spatial overlap in orbitals obtained from the underlying single-electron orbitals by means of a unitary transformation. Second, we show that the optimally tuned RSH functional, which we have previously established for charge-transfer excitations,[53,54] restores the predictive power of TDDFT even for such difficult cases without any external reference data and without any adjustable parameters. The success of this approach is demonstrated on the oligoacene series as well as on related molecules.

II. THEORY OF CHARGE-TRANSFER-LIKE EXCITATIONS

To understand what is a "charge-transfer-like" excitation and how it may arise, consider the general form of the linear-response TDDFT equations based on a RSH functional of the type described above. By straightforward extension of the formalism of ref 55 from a conventional hybrid functional to an RSH one, we obtain

$$\begin{pmatrix} C & D \\ -D & -C \end{pmatrix}\begin{pmatrix} X \\ Y \end{pmatrix} = \hbar\omega\begin{pmatrix} X \\ Y \end{pmatrix} \tag{2}$$

Where X, Y are the electron−hole and hole−electron components, respectively, of the eigenvector in the molecular orbital representation with

$$\begin{aligned} C_{ks\sigma,jt\sigma'} &= (k_\sigma s_\sigma|r_{12}^{-1}|j_{\sigma'}t_{\sigma'}) + (k_\sigma s_\sigma|f_{\sigma\sigma'}^{\gamma}|j_{\sigma'}t_{\sigma'}) \\ &\quad - \delta_{\sigma\sigma'}(k_\sigma j_{\sigma'}|u_\gamma(r_{12})|s_\sigma t_{\sigma'}) + (\epsilon_{s\sigma} - \epsilon_{k\sigma})\delta_{st}\delta_{kj}\delta_{\sigma\sigma'} \end{aligned} \tag{3}$$

and

$$\begin{aligned} D_{ks\sigma,jt\sigma'} &= (k_\sigma s_\sigma|r_{12}^{-1}|j_{\sigma'}t_{\sigma'}) + (k_\sigma s_\sigma|f_{\sigma\sigma'}^{\gamma}|j_{\sigma'}t_{\sigma'}) \\ &\quad - \delta_{\sigma\sigma'}(k_\sigma t_{\sigma'}|u_\gamma(r_{12})|j_{\sigma'}s_\sigma) \end{aligned} \tag{4}$$

where σ, σ' are spin indices, k,j and s,t are, respectively, indices for occupied and unoccupied molecular orbitals, ψ, and eigenvalues, ε, and

$$(k_\sigma s_\sigma|r_{12}^{-1}|j_{\sigma'}t_{\sigma'}) = \iint \frac{\psi_k^\sigma(r)\psi_s^\sigma(r)\psi_j^{\sigma'}(r')\psi_t^{\sigma'}(r')}{|r-r'|}\,d^3r d^3r' \tag{5}$$

$$(k_\sigma s_\sigma|f^\gamma_{\sigma\sigma'}|j_{\sigma'}t_{\sigma'}) = \int \psi^\sigma_k(r)\psi^\sigma_s(r)f^\gamma_{XC}(r;\sigma,\sigma')\psi^{\sigma'}_j(r)\psi^{\sigma'}_t(r)d^3r \quad (6)$$

$$(k_\sigma j_{\sigma'}|u_\gamma(r_{12})|s_\sigma t_{\sigma'}) = \iint \psi^\sigma_k(r)\psi^{\sigma'}_j(r)u_\gamma(|r-r'|)\psi^\sigma_s(r')\psi^{\sigma'}_t(r')d^3rd^3r' \quad (7)$$

where for simplicity all orbitals are assumed to be real and finally, where:

$$u_\gamma(r_{12}) = \frac{erf(\gamma r_{12})}{r} \qquad \bar{u}_\gamma(r) = \frac{erfc(\gamma r_{12})}{r} \quad (8)$$

and $f^\gamma_{XC}(r;\sigma,\sigma')$ is the (semi-)local exchange−correlation kernel arising from the combination of the (semi-)local exchange corresponding to the short-range potential, $\bar{u}_\gamma(r)$, and the (semi-)local correlation. For the simple case of an excitation dominated by a singlet HOMO−LUMO transition, such that the contribution of all other transitions can be neglected, eq 2 reduces to a 2×2 matrix equation involving only the HOMO (H) and LUMO (L) orbitals:

$$\begin{pmatrix} c & d \\ -d & -c \end{pmatrix}\begin{pmatrix} x \\ y \end{pmatrix} = \hbar\omega\begin{pmatrix} x \\ y \end{pmatrix} \quad (9)$$

where, using H(L) for the HOMO (LUMO) index, both of same spin, and $\epsilon_{LH} = \epsilon_L - \epsilon_H$, we have

$$\begin{aligned} c &= \epsilon_{LH} + d + (HL|u_\gamma(r_{12})|HL) - (HH|u_\gamma(r_{12})|LL) \\ d &= (HL|\bar{u}_\gamma(r_{12}) + f^\gamma_{\sigma\sigma}|HL) \end{aligned} \quad (10)$$

which, after straightforward algebra yields

$$(\hbar\omega)^2 = c^2 - d^2 = \epsilon_{cg}(\epsilon_{cg} + 2d) \quad (11)$$

where we defined a "corrected gap", ϵ_{cg}, as

$$\begin{aligned} \epsilon_{cg} &= c - d \\ &= \epsilon_{LH} - (HH|u_\gamma(r_{12})|LL) + (HL|u_\gamma(r_{12})|HL) \end{aligned} \quad (12)$$

In the "extreme CT excitation case" the HOMO and LUMO orbitals are separate, i.e., their spatial overlap is vanishingly small and $|\psi_H(r)||\psi_L(r)| \approx 0$ for all r. In this case, $d = 0$, and the excitation energy equals the corrected gap: $\hbar\omega = \epsilon_{cg} = \epsilon_{LH} - (HH|u_\gamma(r_{12})|LL)$, i.e., the HOMO−LUMO gap corrected by subtracting the long-range Coulomb energy between the electron density and the hole density. When the underlying functional is GGA the correction term is zero, and the excitation energy is equal to the KS HOMO−LUMO gap. This should be compared to the exact optical excitation energy, which in the extreme charge-transfer case is given by the Mulliken limit,[56] IP − EA − $1/R$, where IP is the ionization potential of the donor, EA is the electron affinity of the acceptor, and R is the (large) distance between the electron and the hole. The quantity IP − EA is often referred to as the fundamental gap.[43] Because ϵ_{LH} obtained from a local potential is much smaller than the fundamental gap[43] and because it is independent of R for large R, the charge-transfer excitation energy predicted from TDDFT based on GGA is usually much too low when compared to the experimental gap. We stress that this is a fundamental limitation of the formalism (as opposed to, e.g., an insufficiently accurate choice of parameters). The GGA functional possesses no mechanism that would allow for either increasing the fundamental gap value or including the $1/R$ dependence. With B3LYP the problem is somewhat mitigated, but ϵ_{LH} is still significantly smaller than the fundamental gap and, owing to the fraction of exact exchange, only a fraction of the $1/R$ term is captured. With RSH, ϵ_{LH} can be quantitatively close to the fundamental gap,[57] and the electron−hole binding energy is close to $1/R$ for large R, which immediately explains why charge-transfer excitations are described realistically.

The above explanation of the failure of conventional functionals in describing charge-transfer excitations within linear-response TDDFT cannot be carried over, as is, to a similar phenomenon concerning L_a excitations in oligoacenes, because the HOMO and LUMO spatially overlap strongly, and so there is no charge-transfer to begin with. For example, using B3LYP for anthracene, the spatial overlap between the HOMO and the LUMO orbitals, as defined in eq 1, is 0.88. Thus a different explanation is needed.

There are many cases in the analysis of molecular orbitals where improved intuitive understanding as well as further quantitative analysis is possible with the aid of auxiliary orbitals obtained from the original ones via a unitary transformation. An important and well-known example is the effect of unitary transformations on the degree of orbital localization.[58−61] It is therefore interesting to examine the effect of such transformations on the degree of spatial overlap. As a first step, consider two auxiliary orbitals, ψ_1 and ψ_2, which are obtained from the HOMO and LUMO orbitals via the following simple unitary transformation:

$$\psi_1 = (\psi_H + \psi_L)/\sqrt{2}, \qquad \psi_2 = (\psi_H - \psi_L)/\sqrt{2} \quad (13)$$

In terms of these auxiliary orbitals, eqs 10 and 12 yield

$$\begin{aligned} \epsilon_{cg} &= \epsilon_{LH} - (11|u_\gamma(r_{12})|22) + (12|u_\gamma(r_{12})|12) \\ d &= \frac{1}{4}[(11|\bar{u}_\gamma(r_{12}) + f^\gamma_{\sigma\sigma}|11) + (22|\bar{u}_\gamma(r_{12}) + f^\gamma_{\sigma\sigma}|22) \\ &\quad - 2(11|\bar{u}_\gamma(r_{12}) + f^\gamma_{\sigma\sigma}|22)] \end{aligned} \quad (14)$$

and ϵ_{LH} can be expressed as

$$\begin{aligned} \epsilon_{LH} &= \langle\psi_L|\hat{H}_{DFT}|\psi_L\rangle - \langle\psi_H|\hat{H}_{DFT}|\psi_H\rangle \\ &= -2\langle\psi_1|\hat{H}_{DFT}|\psi_2\rangle \end{aligned} \quad (15)$$

where $\hat{H}_{DFT}$ is the ground-state single-electron Hamiltonian corresponding to the approximate exchange−correlation functional chosen.

Importantly, the GGA-based linear-response TDDFT equations are obtained from eq 9 by considering the limit $\gamma \to 0$, in which $u_\gamma \to 0$ and $\bar{u}_\gamma \to 1/r$. In this limit, eq 14 shows that the corrected gap is equal to the HOMO−LUMO gap, and so the excitation energy is given by

$$(\hbar\omega)^2 = \epsilon_{LH}(\epsilon_{LH} + 2d) \quad (16)$$

Just as we defined the "extreme charge-transfer excitation case" to correspond to completely nonspatialy overlapping HOMO and LUMO orbitals, let us now define the "extreme charge-transfer-like excitation case" to correspond to completely nonspatially overlapping auxiliary orbitals, i.e., $|\psi_1(r)||\psi_2(r)| = 0$ for every r. In practice, in oligoacenes one does not have an extreme charge-transfer-like case, but as shown in Figure 2 for the representative case of anthracene, this scenario is approximately obeyed—the spatial overlap, O_{12}, is 0.30 with B3LYP (0.29 with BNL), compared to 0.88 between the original HOMO and

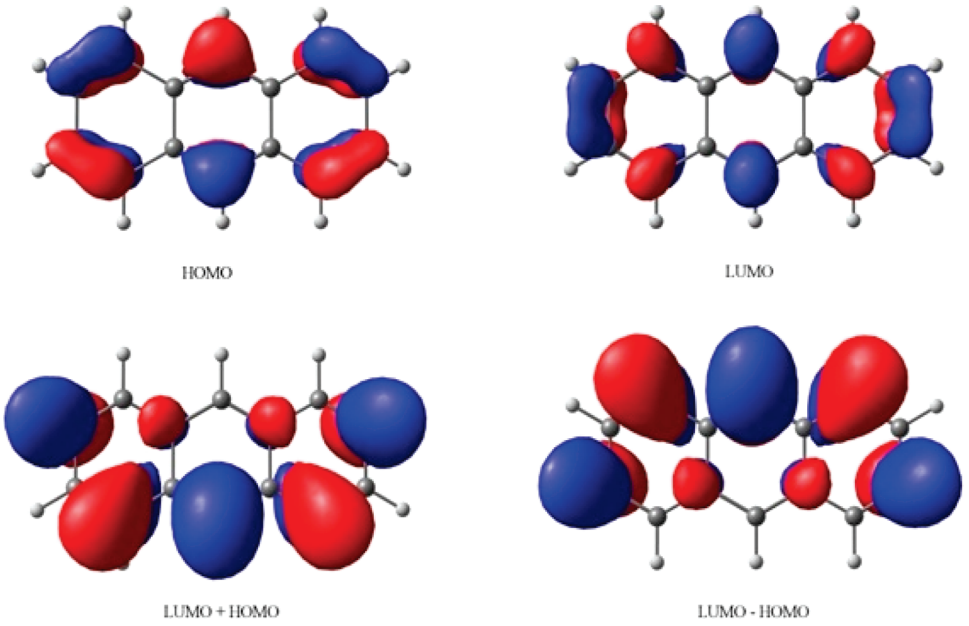

Figure 2. Orbital maps of the HOMO and LUMO orbitals (top) and their normalized sum and difference (bottom) for anthracene, as obtained from the optimally tuned BNL functional.

LUMO. In fact within a simple Hückel picture the zero overlap scenario is fully obeyed. Now, because the GGA Hamiltonian contains no long-range components, we find from eqs 15 and 16 that in this limit, perhaps counterintuitively, both the HOMO−LUMO gap, ϵ_{LH}, and the optical excitation energy, $\hbar\omega$, become vanishingly small! Therefore, the GGA-based calculation necessarily yields very small excitation energies. Just like in the true charge-transfer case, GGA is flawed here. The small spatial overlap of the auxiliary orbitals is a necessity of symmetry and thus inevitably leads to very small gaps, an error for which GGA fundamentally offers no "mechanism" of correction and therefore fails to produce realistic optical gaps. At the same time, the RSH-based calculation, where $\gamma \neq 0$, is saved from such failure because the long-range exchange terms in $\hat{H}_{DFT}$ of eq 15 prevent the HOMO−LUMO gap from vanishing. Furthermore, similar to the CT case, the corrected gap in eq 14 is: $\epsilon_{cg} = \epsilon_{\mathrm{LH}} - (11|u_\gamma(r_{12})|22)$, which differs from the HOMO−LUMO gap precisely by an "exciton binding energy", but between the *auxiliary* orbital charge distributions, $|\psi_1(r)|^2$ and $|\psi_2(r)|^2$.

The similarities and differences between a charge-transfer-like and a true charge-transfer excitation are now clear: In both types of excitations, the serious errors that GGA-based calculations may arise from the presence of weakly spatially overlapping orbitals and the absence of nonlocality in the exchange−correlation kernel. And in both types of excitations, use of a Fock exchange term results in excitonic terms that correctly describe the physics of the transition. But in charge-transfer-like excitations, unlike in true charge-transfer ones, all this does not involve the orbitals obtained directly from the ground-state DFT calculation but rather a unitary transformation thereof. Consequently, the charge-transfer-like character cannot be exposed by considering only the untransformed orbitals or the density difference induced by the excitation.

We note that the above-scenario is clearly just one out of an entire family of charge-transfer-like scenarios, in which weakly spatially overlapping orbitals are obtained via a unitary transformation of the molecular ones. For example, the pertinent unitary transformation does not have to be one of a 45° rotation in the orbital space. In this sense, the true charge-transfer excitation is simply the one obtained with the trivial (identity) unitary transformation. Furthermore, if the transition is dominated by more than one pair of orbitals, the requisite unitary matrix will be larger. An interesting special case of the latter scenario, analyzed in detail by Hieringer and Görling,[62−64] is that of excitations in a spatially separated homodimer. There, the transition is dominated by four orbitals, two corresponding to a linear combination of the HOMO of each monomer and two corresponding to a linear combination of the LUMO of each monomer. Also in this case the excitation does not involve charge-transfer that can be deduced from density differences, and yet linear-response TDDFT based on GGA fails. But a 4 × 4 unitary transformation exposes the absence of spatial overlap between the HOMO of one monomer and the LUMO of the other as the true source of this failure.[65]

Determining whether, and which, unitary transformation minimizes the spatial overlap of pertinent orbitals and whether weakly spatially overlapping orbitals can be obtained, then emerges as a path to deciding a priori whether a TDDFT failure associated with charge-transfer-like excitations may occur, thus answering the first challenge posted by Richard and Herbert.[51]

We further note that Peach et al.[28] introduced a "spatial overlap measure", Λ, to be used as a diagnostic tool in a general scenario involving multiple molecular orbitals:

$$\Lambda = \frac{\sum_{ia} \kappa_{ia}^2 O_{ia}}{\sum_{ia} \kappa_{ia}^2} \tag{17}$$

where $\kappa_{ia} = X_{ia} + Y_{ia}$ (**X** and **Y** are the vector solutions of the linear-response TDDFT equations defined in eq 2 and O_{ia} is the spatial overlaps defined in eq 1 with ψ_1 the i^{th} (occupied) molecular orbital and ψ_2 the a^{th} (unoccupied) molecular orbital. A value of Λ that is too small indicates a charge-transfer situation, warning the user not to rely on standard functionals. The above discussion immediately explains the observation[50,51] that Λ does not "sound the alarm" when a charge-transfer-like situation

arises, because the spatial overlap between the original orbitals is not small. However, the present work suggests that a relatively straightforward remedy is to seek the unitary transformation that minimizes a spatial overlap criterion such as that of Peach et al., then use as a diagnostic warning tool the value computed using the orbitals obtained with this unitary transformation.

III. PREDICTING CHARGE-TRANSFER-LIKE EXCITATIONS FROM AN OPTIMALLY TUNED RANGE-SEPARATED HYBRID FUNCTIONAL

Having laid out the general principles of charge-transfer-like excitations in the previous section, we make no attempt here at creating a comprehensive catalogue of charge-transfer-like scenarios. Instead, we move to the second and practically more pertinent challenge raised by Richard and Herbert:[51] How can the predictive power of TDDFT, even in the presence of such "difficult cases", be restored? eq 14 and its associated analysis, together with the excellent numerical results of Wong and Hsieh[50] and of Richard and Herbert,[51] clearly suggest the use of an RSH functional. However, a serious difficulty remains, which is the choice of the range separation parameter, γ. The above-mentioned previous TDDFT studies of oligoacenes with RSH functionals have deduced appropriate values for γ from either coupled cluster or experimental data. While this is a perfectly valid approach, it limits the application of the method to new and unknown systems, especially given that the best choice of γ is known to generally vary with system.[30,54,57,66,67]

In previous work on inter- and intramolecular charge-transfer excitations,[53,54] we have shown that full predictive power can be obtained by *optimally tuning* the range-separation parameter, γ. The suggested tuning procedure has been discussed in detail elsewhere.[53,54,57] Briefly, as mentioned above, in the limit of an infinite donor−acceptor separation, the lowest excitation energy of true charge-transfer systems reduces to the difference between the ionization potential of the donor and the electron affinity of the acceptor. Therefore, these quantities must be well predicted by ground-state DFT eigenvalues if the computation is to reduce to the correct limit. If the exact exchange−correlation functional is used, then the DFT version of Koopmans' theorem establishes that the highest-occupied eigenvalue is equal and opposite to the ionization potential.[68−70] This implies that an optimal choice for obtaining the correct ionization potential of an N electron system from the highest occupied RSH eigenvalue is to enforce Koopmans' theorem, i.e., to find γ such that

$$-\epsilon_{\mathrm{H}}^{\gamma}(N) = I^{\gamma}(N) \equiv E_{gs}(N-1;\gamma) - E_{gs}(N;\gamma) \qquad (18)$$

where $I^{\gamma}(M)$ is the ionization potential of an M electron system, calculated as a ground-state energy difference, $\epsilon_{\mathrm{H}}^{\gamma}(M)$ is the HOMO energy, and $E_{gs}(M;\gamma)$ is the ground-state energy of an M electron system. For determining the electron affinity, we employ Koopmans' theorem also for the ionization potential of the negatively charged system, which, barring relaxation effects, is the same as electron affinity of the original system. Because there is one parameter but two conditions, we seek the γ that minimizes the overall deviation expressed in the target function:

$$J^2(\gamma) = (\epsilon_{\mathrm{H}}^{\gamma}(N) + I^{\gamma}(N))^2 + (\epsilon_{\mathrm{H}}^{\gamma}(N+1) + I^{\gamma}(N+1))^2 \qquad (19)$$

The down-side of using eq 19 is that the optimal value of γ needs to be determined for each system of interest separately. Among other things, this does not allow for size consistency of the functional. But a crucial observation as far as predictive power is concerned is that using eq 19 to choose the optimal γ does not require any empirical input and that the procedure contains no adjustable parameters. In other words, eq 19 is a *tuning* procedure but not a *fitting* procedure. Furthermore, it is based on upholding a physical criterion (enforcing a known and pertinent limit the exact functional must obey) rather than on semiempirical considerations. In the following, we examine whether the same approach is also useful for charge-transfer-like scenarios.

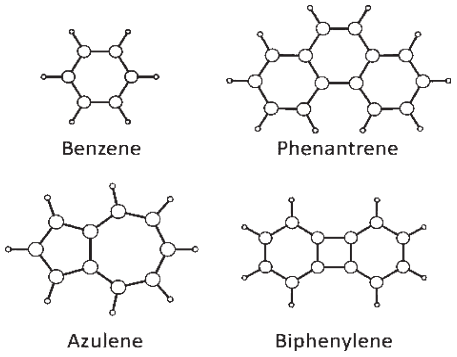

Figure 3. Schematic representation of benzene, azulene, phenanthrene, and biphenylene.

All RSH calculations presented in this work were performed using the Baer, Neuhauser, and Livshits (BNL) functional,[30,47] as implemented in version 3.2 of Q-CHEM.[71] In this functional, the long-range exchange term is a Fock-like term based on the $r^{-1}\,\mathrm{erf}(\gamma r)$ potential, whereas the short-range exchange is a local expression, due to Toulouse et al,[72] which is based on the $r^{-1}\,\mathrm{erfc}(\gamma r)$ potential. The correlation term is the standard Lee, Yang, and Parr (LYP) expression.[73] All BNL calculations were performed using the correlation-consistent triple-ζ basis set, cc-PVTZ,[74] which was carefully tested for convergence. All ground-state structures were optimized within a B3LYP calculation. For the oligoacenes, we used the coordinates provided by Wong and Hsieh.[50] For other molecules, we performed our own optimization.

For oligoacenes, we have previously shown[57] that optimal tuning using eq 19 (or using eq 18 for molecules without a positive electron affinity) does yield a quantitatively accurate prediction for the fundamental gaps (i.e., differences between the ionization potential and the electron affinity) throughout the series. Importantly, we found that the optimally tuned γ values decrease monotonically with system size; for naphthalene, the optimal value is 0.28, whereas for hexacene it is a significantly smaller 0.19. We have interpreted this physically as being due to the increase of electron delocalization with increasing size of this conjugated system, which renders the necessary weight of exact exchange smaller.

The TDDFT results obtained from the optimally tuned BNL calculations for the ^1L_a and ^1L_b excitation energies are shown in Figure 1, along with the previously discussed GGA and B3LYP results and the reference CC2 values. Unlike the GGA or B3LYP results, the optimally tuned BNL calculations are on par with those of the CC2 reference results for the ^1L_a excitation energy. Specifically, the GGA and B3LYP results significantly underestimate the CC2 ones by a mean value of 0.74 and 0.47 eV, respectively. But the optimally tuned BNL results only

Table 1. Lowest Singlet Excitations for Benzene, Azulene, Phenanthrene, and Biphenylene[a]

molecule	BP86	B3LYP	BNL*	CC2[76]	dominant transition	optimal γ	transition dipole moment
				"Well-Predicted" Excitation			
benzene	5.32	5.47	5.50	5.27	H→L H-1→L+1	0.310	0.00
azulene	2.34	2.41	2.35	2.31	H→L	0.262	0.37 (short axis)
phenanthrene	3.66	3.98	4.19	4.04	H-1→L H→L+1	0.247	0.10 (short axis)
biphenylene	3.67	3.93	4.11	3.88	H-1→L H→L+1	0.253	1.08 (long axis)
				"Poorly Predicted" Excitation			
benzene	6.07	6.16	6.40	6.56	H→L+1 H-1→L	0.310	0.00
azulene	3.49	3.64	3.79	3.95	H-1→L H→L+1	0.262	0.19 (long axis)
phenanthrene	3.92	4.22	4.57	4.70	H→L H-1→L+1	0.247	0.85 (long axis)
biphenylene	3.14	3.32	3.57	3.69	H→L	0.253	0.00

[a] Excitation energies, in eV, obtained from TDDFT calculations with the BP86 GGA functional, the B3LYP standard hybrid functional, and the optimally tuned BNL range-separated hybrid functional are compared to reference CC2 values, taken from ref 71. Transitions where TDDFT with B3LYP provides satisfactory agreement with CC2 results ("well-predicted" excitations) are grouped separately from transitions where agreement was not satisfactory ("poorly predicted" excitations). Also given are the dominating transitions (where "H" stands for HOMO and "L" for LUMO) as well the optimal range-separation parameter, γ, and the resulting dipole moment (in atomic units) for the optimally tuned BNL calculations.

underestimate the CC2 ones by 0.15 eV, which is within the accepted error margin of either approach.[54,75] Exactly as in true charge-transfer excitations, the fact that B3LYP contains a *fraction* of exact exchange has mitigated, but not solved, the quantitative failure resulting from the charge-transfer-like character of the excitation. We note that in refs 50 and 51 a smaller mean average error between RSH-based and CC2 results, of ∼0.05 eV, was obtained with some of the RSH-based functionals used. Some of this difference is likely due to details of the local exchange and correlation used. However, given the limits of accuracy of the CC2 reference data themselves, our results are on par with the previous ones, without recourse to empirical parameters.

Equally importantly, the transition from B3LYP to optimally tuned BNL functional does not compromise accuracy for the ^1L_b excitation energies, where the mean error with B3LYP and BNL is 0.04 and 0.09 eV, respectively (GGA produces a less satisfactory, but perhaps tolerable, mean error of 0.28 eV). In other words, one obtains quantitative agreement with experiment (∼0.1−0.2 eV), irrespective of the presence or absence of charge-transfer-like characteristics. Again, this is on par with the previous RSH-based results of refs 50 and 51 without recourse to empiricism. Thus, the second challenge raised by Richard and Herbert—achieving true predictive power—can be met even without going through the mathematical tedium of identifying the unitary transformation which minimizes the spatial overlap of pertinent orbitals, from which the nature of the failure of standard functionals becomes apparent.

For further confirmation of our computational approach, we performed similar calculations for four additional molecules: benzene, azulene, phenanthrene, and biphenylene, shown in Figure 3. These four molecules were chosen for several reasons. First, these molecules represent scenarios that are more general than that afforded by the oligacene series. Benzene is of higher symmetry, azulene is a nonalternant hydrocarbon, phenanthrene is a nonlinear hydrocarbon, and biphenylene exhibits antiaromaticity. Second, Falden et al. recently provided wave function-based reference values for these molecules (of which we use the CC2 results for consistency).[76] Third, as summarized in Table 1, when using B3LYP each molecule exhibits both "well-predicted" low-lying excitation energies (i.e., showing differences of ∼0.1−0.2 eV from the CC2 values) and "poorly-predicted" low-lying excitation energies (i.e., showing differences of ∼0.3−0.5 eV from the CC2 values).

Table 1 shows that the optimized BNL results provide for a balanced and satisfactory level of accuracy (a mean error of ∼0.15 eV for both types of excitations), despite the different nature of both the problematic and the nonproblematic transitions. Furthermore, as also shown in Table 1, each molecule possesses its own different optimally tuned range-separation parameter, underscoring the importance of optimal, molecule-specific tuning. They also lend further support our above presented theory of charge-transfer-like excitation: For azulene, unlike its alternant analogue, naphthalene, the HOMO−LUMO dominated transition is well-described by B3LYP. And indeed, for azulene no unitary transformation of the HOMO and LUMO orbitals was found to result in weakly spatially overlapping orbitals. The minimal spatial overlap was found to be 0.55 with B3LYP (0.57 with BNL), for the original HOMO and LUMO, and any 2 × 2 unitary transformation of the HOMO and LUMO orbitals was found to merely increase this number. This again underscores the diagnostic role unitary transformations play in uncovering whether, and which, excitations may be prone to charge-transfer-like errors. At the same time, it shows that with an optimally tuned RSH functional, such diagnostics are not essential to obtaining quantitatively predictive results.

IV. CONCLUSIONS

In conclusion, we have addressed the conundrum posed by "charge-transfer excitations in disguise". We have shown that such excitations are due to a small spatial overlap in orbitals obtained from the underlying single-electron orbitals by means of a unitary transformation. Furthermore, we have shown that, as in true charge-transfer excitations, this necessarily results in failure of linear-response TDDFT with standard functionals. Second, we show that with optimal tuning of a range-separated hybrid functional, so as to enforce the DFT version of Koopmans' theorem, the predictive power of TDDFT is restored even for such difficult cases without any external reference data and without any adjustable parameters. We demonstrated the success of this approach on the oligoacene series and on related hydrocarbons. This resolves a long-standing question in TDDFT and extends the scope of molecules and systems to which TDDFT can be applied in a predictive manner.

AUTHOR INFORMATION

Corresponding Authors

*E-mail: leeor.kronik@weizmann.ac.il; roi.baer@huji.ac.il.

Author Contributions

§These authors contributed equally

ACKNOWLEDGMENT

Work in Rehovoth was supported by the Israel Science Foundation and the Lise Meitner Minerva Center for Computational Chemistry. Work in Jerusalem was supported by the Israel Science Foundation.

REFERENCES

(1) Runge, E.; Gross, E. K. U. *Phys. Rev. Lett.* **1984**, *52*, 997–1000.
(2) Marques, M.; Rubio, A.; Ullrich, C. A.; Burke, K.; Nogueira, F.; Gross, A. *Time-dependent density functional theory*; Springer: Berlin, Germany, 2006.
(3) Onida, G.; Reining, L.; Rubio, A. *Rev. Mod. Phys.* **2002**, *74*, 601–659.
(4) Burke, K.; Werschnik, J.; Gross, E. K. U. *J. Chem. Phys.* **2005**, *123*, 062206.
(5) Elliott, P.; Furche, F.; Burke, K. In *Excited states from time-dependent density functional theory*; Wiley: Hoboken, NJ, 2009; Vol. 26.
(6) Kohn, W.; Sham, L. J. *Phys. Rev.* **1965**, *140*, A1133.
(7) Perdew, J. P.; Kurth, S. In *A Primer in Density Functional Theory*; Springer: Berlin, Germany, 2003.
(8) Becke, A. D. *J. Chem. Phys.* **1993**, *98*, 1372–1377.
(9) Stephens, P. J.; Devlin, F. J.; Chabalowski, C. F.; Frisch, M. J. *J. Phys. Chem.* **1994**, *98*, 11623–11627.
(10) Chelikowsky, J. R.; Kronik, L.; Vasiliev, I. *J. Phys.: Condens. Mater.* **2003**, *15*, R1517–R1547.
(11) Silva, M. R.; Schreiber, M.; Sauer, S. P. A.; Thiel, W. *J. Chem. Phys.* **2008**, 129.
(12) Adamo, C.; Scuseria, G. E.; Barone, V. *J. Chem. Phys.* **1999**, *111*, 2889–2899.
(13) Furche, F.; Ahlrichs, R. *J. Chem. Phys.* **2002**, *117*, 7433–7447.
(14) Grimme, S.; Parac, M. *ChemPhysChem* **2003**, *4*, 292–295.
(15) Platt, J. R. *J. Chem. Phys.* **1949**, *17*, 484.
(16) Becke, A. D. *Phys. Rev. A* **1988**, *38*, 3098–3100.
(17) Perdew, J. P. *Phys. Rev. B* **1986**, *33*, 8822–8824.
(18) Parac, M.; Grimme, S. *Chem. Phys.* **2003**, *292*, 11–21.
(19) Kuhlman, T. S.; Mikkelsen, K. V.; Møller, K. B.; Sølling, T. I. *Chem. Phys. Lett.* **2009**, *478*, 127–131.
(20) Malloci, G.; Mulas, G.; Cappellini, G.; Joblin, C. *Chem. Phys.* **2007**, *340*, 43–58.
(21) Heinze, H. H.; Goerling, A.; Roesch, N. *J. Chem. Phys.* **2000**, *113*, 2088–2099.
(22) Marian, C. M.; Gilka, N. *J. Chem. Theory Comput.* **2008**, *4*, 1501–1515.
(23) Wang, Y. L.; Wu, G. S. *Int. J. Quantum Chem.* **2008**, *108*, 430–439.
(24) Although comparison to experimental results obtained in solution results in similar trends,[14] here we prefer the comparison to single-molecule CC2 results in order to avoid issues related to modeling of solvent effects.
(25) Dreuw, A.; Head-Gordon, M. *J. Am. Chem. Soc.* **2004**, *126*, 4007–4016.
(26) Tozer, D. J. *J. Chem. Phys.* **2003**, *119*, 12697–12699.
(27) Autschbach, J. *ChemPhysChem* **2009**, *10*, 1757–1760.
(28) Peach, M. J. G.; Benfield, P.; Helgaker, T.; Tozer, D. J. *J. Chem. Phys.* **2008**, *128*, 044118.
(29) Ziegler, T.; Seth, M.; Krykunov, M.; Autschbach, J.; Wang, F. *(Theochem) J. Mol. Struct.* **2009**, *914*, 106–109.
(30) Livshits, E.; Baer, R. *Phys. Chem. Chem. Phys.* **2007**, *9*, 2932–2941.
(31) Dreuw, A.; Weisman, J. L.; Head-Gordon, M. *J. Chem. Phys.* **2003**, *119*, 2943–2946.
(32) Wong, B. M.; Cordaro, J. G. *J. Chem. Phys.* **2008**, *129*, 214703.
(33) Chai, J. D.; Head-Gordon, M. *J. Chem. Phys.* **2008**, *128*, 084106.
(34) Tawada, Y.; Tsuneda, T.; Yanagisawa, S.; Yanai, T.; Hirao, K. *J. Chem. Phys.* **2004**, *120*, 8425–8433.
(35) Lange, A. W.; Rohrdanz, M. A.; Herbert, J. M. *J. Phys. Chem. B* **2008**, *112*, 6304–6308.
(36) Epifanovsky, E.; Polyakov, I.; Grigorenko, B.; Nemukhin, A.; Krylov, A. I. *J. Chem. Theory Comput.* **2009**, *5*, 1895–1906.
(37) Govind, N.; Valiev, M.; Jensen, L.; Kowalski, K. *J. Phys. Chem. A* **2009**, *113*, 6041–6043.
(38) Akinaga, Y.; Ten-No, S. *Int. J. Quantum Chem.* **2009**, *109*, 1905–1914.
(39) Andzelm, J.; Rinderspacher, B. C.; Rawlett, A.; Dougherty, J.; Baer, R.; Govind, N. *J. Chem. Theory Comput.* **2009**, *5*, 2835.
(40) Mohammed, A.; Agren, H.; Norman, P. *Phys. Chem. Chem. Phys.* **2009**, *11*, 4539–4548.
(41) Pastore, M.; Mosconi, E.; De Angelis, F.; Gratzel, M. *J. Phys. Chem. C* **2010**, *114*, 7205–7212.
(42) Kerkines, I. S. K.; Petsalakis, I. D.; Theodorakopoulos, G.; Rebek, J. *J. Phys. Chem. A* **2011**, *115*, 834–840.
(43) Kümmel, S.; Kronik, L. *Rev. Mod. Phys.* **2008**, *80*, 3–60.
(44) Leininger, T.; Stoll, H.; Werner, H.-J.; Savin, A. *Chem. Phys. Lett.* **1997**, *275*, 151–160.
(45) Yanai, T.; Tew, D. P.; Handy, N. C. *Chem. Phys. Lett.* **2004**, *393*, 51–57.
(46) Iikura, H.; Tsuneda, T.; Yanai, T.; Hirao, K. *J. Chem. Phys.* **2001**, *115*, 3540–3544.
(47) Baer, R.; Neuhauser, D. *Phys. Rev. Lett.* **2005**, *94*, 043002.
(48) Henderson, T. M.; Janesko, B. G.; Scuseria, G. E. *J. Chem. Phys.* **2008**, *128*, 194105.
(49) Vydrov, O. A.; Scuseria, G. E. *J. Chem. Phys.* **2006**, *125*, 234109.
(50) Wong, B. M.; Hsieh, T. H. *J. Chem. Theory Comput.* **2010**, *6*, 3704–3712.
(51) Richard, R. M.; Herbert, J. M. *J. Chem. Theory Comput.* **2011**, *7*, 1296–1306.
(52) As explained above, here we take charge-transfer to imply a small spatial overlap between the initial and final state of the excited electron. In valence-bond language, ^1L_a transitions are "ionic" whereas ^1L_b transitions are "covalent", hinting at charge transfer.[14,50] However the spatial overlap of the initial and final state is still significant.
(53) Stein, T.; Kronik, L.; Baer, R. *J. Am. Chem. Soc.* **2009**, *131*, 2818–2820.
(54) Stein, T.; Kronik, L.; Baer, R. *J. Chem. Phys.* **2009**, *131*, 244119–5.
(55) Tretiak, S.; Chernyak, V. *J. Chem. Phys.* **2003**, *119*, 8809–8823.
(56) Mulliken, R. S. *J. Am. Chem. Soc.* **1950**, *72*, 600–608.

(57) Stein, T.; Eisenberg, H.; Kronik, L.; Baer, R. *Phys. Rev. Lett.* **2010**, *105*, 266802.
(58) Marzari, N.; Vanderbilt, D. *Phys. Rev. B* **1997**, *56*, 12847–12865.
(59) Foster, J. M.; Boys, S. F. *Rev. Mod. Phys.* **1960**, *32*, 300.
(60) Edmiston, C.; Ruedenberg, K. *Rev. Mod. Phys.* **1963**, *35*, 457.
(61) Körzdörfer, T.; Kümmel, S.; Mundt, M. *J. Chem. Phys.* **2008**, *129*, 014110.
(62) Hieringer, W.; Goerling, A. *Chem. Phys. Lett.* **2006**, *419*, 557–562.
(63) Dreuw, A.; Head-Gordon, M. *Chem. Phys. Lett.* **2006**, *426*, 231–233.
(64) Hieringer, W.; Goerling, A. *Chem. Phys. Lett.* **2006**, *426*, 234–236.
(65) Kuhlman et al. (ref 19) have previously speculated on a possible connection between the failure observed in oligoacenes and that observed in the symmetric dimer but have not provided a mathematical analysis of the similarities and differences between the two cases.
(66) Baer, R.; Livshits, E.; Neuhauser, D. *Chem. Phys.* **2006**, *329*, 266–275.
(67) Livshits, E.; Baer, R. *J. Phys. Chem. A* **2008**, *112*, 12789–12791.
(68) Perdew, J. P.; Parr, R. G.; Levy, M.; Balduz, J. L. *Phys. Rev. Lett.* **1982**, *49*, 1691–1694.
(69) Almbladh, C.-O.; von-Barth, U. *Phys. Rev. B* **1985**, *31*, 3231–3244.
(70) Cohen, A. J.; Mori-Sanchez, P.; Yang, W. T. *Phys. Rev. B* **2008**, *77*, 115123.
(71) Shao, Y.; Molnar, L. F.; Jung, Y.; Kussmann, J.; Ochsenfeld, C.; Brown, S. T.; Gilbert, A. T. B.; Slipchenko, L. V.; Levchenko, S. V.; O'Neill, D. P.; DiStasio, R. A.; Lochan, R. C.; Wang, T.; Beran, G. J. O.; Besley, N. A.; Herbert, J. M.; Lin, C. Y.; Van Voorhis, T.; Chien, S. H.; Sodt, A.; Steele, R. P.; Rassolov, V. A.; Maslen, P. E.; Korambath, P. P.; Adamson, R. D.; Austin, B.; Baker, J.; Byrd, E. F. C.; Dachsel, H.; Doerksen, R. J.; Dreuw, A.; Dunietz, B. D.; Dutoi, A. D.; Furlani, T. R.; Gwaltney, S. R.; Heyden, A.; Hirata, S.; Hsu, C. P.; Kedziora, G.; Khalliulin, R. Z.; Klunzinger, P.; Lee, A. M.; Lee, M. S.; Liang, W.; Lotan, I.; Nair, N.; Peters, B.; Proynov, E. I.; Pieniazek, P. A.; Rhee, Y. M.; Ritchie, J.; Rosta, E.; Sherrill, C. D.; Simmonett, A. C.; Subotnik, J. E.; Woodcock, H. L.; Zhang, W.; Bell, A. T.; Chakraborty, A. K.; Chipman, D. M.; Keil, F. J.; Warshel, A.; Hehre, W. J.; Schaefer, H. F.; Kong, J.; Krylov, A. I.; Gill, P. M. W.; Head-Gordon, M. *Phys. Chem. Chem. Phys.* **2006**, *8*, 3172–3191.
(72) Toulouse, J.; Savin, A.; Flad, H. J. *Int. J. Quantum Chem.* **2004**, *100*, 1047–1056.
(73) Lee, C.; Yang, W.; Parr, R. G. *Phys. Rev. B* **1988**, *37*, 785–789.
(74) Dunning, T. H. *J. Chem. Phys.* **1989**, *90*, 1007–1023.
(75) Schreiber, M.; Silva-Junior, M. R.; Sauer, S. P. A.; Thiel, W. *J. Chem. Phys.* **2008**, *128*, 134110–25.
(76) Falden, H. H.; Falster-Hansen, K. R.; Bak, K. L.; Rettrup, S.; Sauer, S. P. A. *J. Phys. Chem. A* **2009**, *113*, 11995–12012.